



China Active Faults Database and its web system

Xiyan Wu¹, Xiwei Xu^{2,3}, Guihua Yu¹, Junjie Ren³, Xiaoping Yang¹, Guihua Chen¹, Chong Xu³, Keping Du⁴, Xiongnan Huang¹, Haibo Yang¹, Kang Li³, Haijian Hao¹

5 ¹ State Key Laboratory of Earthquake Dynamics, Institute of Geology, China Earthquake Administration, Beijing 100029, China

² School of Earth Sciences and Resources, China University of Geosciences, Beijing 100083, China

³ National Institute of Natural Hazards, Ministry of Emergency Management of China, Beijing, 100085, China

⁴ Beijing Normal University, Beijing 100091, China

10 *Correspondence to:* Xiwei Xu (xiweixu@vip.sina.com)

Abstract. Active faults are potential destructive earthquake sources and also the most serious strips of earthquake disasters in the future. Studies and investigations of active faults are necessary for earthquake hazard reduction. This study presents a nation-scale database of the active faults for China and its adjacent regions along with associated web-based query system. This database is an updated version of the active faults data included in the “Seismotectonic Map of China and its Adjacent Regions (1:4 000 000),” which is one of the four essential maps of the mandatory Chinese standard GB/T 18306-2015 Seismic Ground Motion Parameter Zonation Maps of China. The data update and integration are based on the latest 20-year region-scale active fault survey data (1:250 000 – 1:50 000). Those data include geophysical probing, drill logging, offset-landform measuring and sample dating, as well as geometric and kinematic parameters of exposed and blind faults, paleo-earthquake sequences, and recurrence intervals, and have been obtained and analyzed using the same technical standard framework and reviewed by expert panels in the field and laboratory. The database can be interrogated using a Web Geographic Information System (GIS) application, which provides browsing, inquiring, analyzing, and downloading functions on a web browser. The system also publishes the Open Geospatial Consortium (OGC) Web Feature Service and OGC Web Map Service of active fault data. Users can add map layers and download fault data in the OGC-compliant GIS software for further analyses via these services. The Chinese government, research institutions, and companies have widely used the active faults data from the previous versions of the Database. The database is available at <https://doi.org/10.12031/activefault.china.400.2022.db> (Xu, 2022) and via the Web System (CEFIS (V2), 2023; CAFD WFS). It is downloadable through diverse platforms and clients as introduced in Sections 4.3.2 and 4.4.

1 Introduction

30 Earthquake is one of the most dangerous natural disasters in the world. A close relationship exists between the strong or great earthquake and the spatial feature of an active fault. In generally an earthquake of magnitude (M) ≥ 7.0 often occur on



active faults or overlap with them. In statistics, almost all $M \geq 8.0$ earthquakes and most $M=7.0-7.9$ earthquakes in China have been recorded to rupture parts of the main boundary fault around an active block in China (Xu and Deng, 1996; Deng et al., 2003; Zhang et al., 2003; Xu et al., 2016a). Furthermore, more than 70 co-seismic surface rupture zones generated by the great earthquakes are spatially coincident with the known active faults (Xu and Deng, 1996; Zhang et al., 2003; Xu et al., 2017). Therefore, determining the geometries and locations of the active faults and their slip rates, and then constructing a corresponding database of the active faults is essential for preventing the social and economic losses caused by the destructive earthquakes and protecting lives and property (Xu et al., 2002, 2006; Tian et al., 2006).

Some countries have constructed comprehensive active faults databases in the past twenty years (Haller et al., 2004; Basili et al., 2008, 2021; Yoshioka and Miyamoto, 2011; Ganas et al., 2013; Langridge et al., 2016; Emre et al., 2018, Maldonado et al., 2021; Williams et al., 2022), some of which are publicly available. For example, the National Institute of Geophysics and Volcanology of Italy published the Database of Individual Seismogenic Source (DISS) in the 2000s. The latest version of DISS is 3.3.0 (Valensise and Pantatosti, 2001; Basili et al., 2008, 2021). This latest database includes ~200 faults. The U.S. Geological Survey established the first nationwide compilation of the U.S. Quaternary Faults and Folds Database in the early 2000s, which contained ~2000 faults (Haller et al., 2004).

China is in the convergence zone of the Indian, Eurasian and Pacific Plates where many seismogenic active faults have developed, and becomes one of the countries with the most severe earthquake disasters at present and also in history. The earliest historical earthquake records worldwide were obtained in China. An active faults database of China is essential for the in-depth studies of regional crustal kinematic characteristics, intraplate earthquake features, and earthquake disaster mitigation action programme. The China Earthquake Administration organized a compilation of a 1:4 000 000-scale active tectonic database (Qu, 2008) in the 2000s. This database was based on Deng's 1:4 000 000-scale active tectonic map and included more than 800 active faults and 48 active folds (Deng et al., 2002, 2007). It summarized researches on active faults carried out in China before 2002 AD. However, many active faults were not well identified or studied at that time. A large amount of survey work should be carried out because China is situated in the Circum-Pacific and Himalayan-Mediterranean seismic zones, producing strong neotectonic and frequent seismic activities. To determine the accurate position and slip age of active fault, which is of capable to generate destructive earthquakes, a series of active fault surveys and mapping projects has been launched since 2007 in China. These projects consist of the following: 1) fundamental maps and data collection for national earthquake hazards prevention, such as the 5th generation "Seismic ground motion parameters zonation map of China" (China mandatory standard GB/T 18306-2015); 2) active fault prospecting in urban regions and their earthquake risk assessments, such as "Urban active fault experimental prospecting" (2001–2003) and "Seismo-active-fault prospecting technology system in China" (2004–2008); 3) seismo-active-fault survey and mapping, such as "The Himalayan Plan: active fault mapping at scale of 1:50 000 in the north China tectonic region and along the North-South seismic zone" and "Earthquake risk assessment of active faults in the key earthquake surveillance and prevention areas"; 4) other scientific researches. Accurate geometric and activity kinematic parameters as well as mechanical property for the studied active faults are identified in those projects by systematically analyzing the published scientific literature, remote sensing data, field



surveys, and dating samples from geological profiles, trenches and boreholes (Xu et al., 2015). A professional panel then review the obtained parameters and rechecked the final results to ensure reliability. In every project, an overall prospecting-and-surveying-process database is built to record all project data from beginning to end. Those project databases include data associated with the geophysical prospecting, drilling, offset-landform measuring and sample dating, geometric and kinematic
70 parameters of the exposed and blind faults, paleo-earthquakes, their occurrence ages and recurrence intervals. The data types include two-dimensional Geographic Information System (GIS) data, photographs, geological interpretation pictures, geophysical prospecting data, electronic literature, and scientific reports. By the end of 2019, the project's total amount of data was reached 7 Terabytes.

The China Active Faults Database (CAFD) is a comprehensive geospatial database that summarizes the most reliable results
75 of the abovementioned projects, based on two basic databases with accuracy of 1:50,000 single active fault mappings and 1:250,000 regional active fault distribution. The web-based query system is open to the public and shares the latest version of China's active fault database. Section 2 introduces the history and development of nationwide active fault maps and databases in China. Data acquisition, data resources, data processing, database compilation, and data quality are discussed in Section 3. In addition, several classical application cases are presented to demonstrate the extensive use of the database. The
80 construction, function, performance, and usage of the web-based active fault query system are described in Section 4. System users can browse and query fault information, obtain data from the Web Feature Service (WFS) and Web Map Service (WMS) servers in GIS software (such as ArcGIS and QGIS), and add active faults as layers in their web applications.

2 Nationwide active fault maps and databases

Different organizations and experts compiled the nationwide active tectonics and fault maps of China during different
85 periods. Those maps, such as the "Spatial distribution map of active tectonics and strong earthquakes in China (1:3 000 000)" (NESZMT, 1976), "Map of the major tectonic-system activity and strong earthquakes epicenter distribution in China (1:6 000 000)" (NEIZMT, 1978), "Seismotectonic map of China (1:4 000 000)" (GICEA, 1979), and "Lithospheric dynamics map of China and adjacent sea area (1:4 000 000)" (Ma, 1987), had systematically summarized the latest research achievements at a specific periods.

90 In the past ten years, the most influential nationwide active fault maps have been "The active tectonic map of China (1:4 000 000)" (Deng et al., 2007) and "Seismotectonic Map in China and its Adjacent Regions (1:4 000 000)" (SMCAR; Xu et al., 2016). Deng et al. (2007) systematically summarized the classical tectonic characteristics, such as the latest slip rate and age of faults, historically strong earthquake activity, and co-seismic surface ruptures in mainland China and adjacent sea areas. In addition to the print edition, a geospatial database based on the map (Deng et al., 2007) was constructed (Qu et al., 2008). It
95 was widely shared with scientists, specialists, and the public over the past ten years, although not available online. Its earlier version was integrated into the early version of Active Faults of Eurasia Database (Trifonov et al., 2004), of which an updated version was published in 2022 (Zelenin et al., 2022). Currently, it can be freely downloaded online (NEDC (sub-



center in IG, CEA), 2023), and scientists have updated this map based on new findings. For example, Wu et al. (2018) compiled a “spatial distribution map of active faults in China and its adjacent sea areas (1:5 000 000) (2018)” by
100 synthesizing past decadal publications in Chinese and English and 15-year research on active faults achieved by the Institute of Geomechanics in the Chinese Academy of Geological Sciences.

The SMCAR (Xu et al., 2016) is a subproject of the 5th generation “Seismic ground motion parameter zonation maps of China” and one of the four essential maps of the Chinese mandatory standard GB/T 18306-2015. This standard aims to develop seismic fortification criteria for anti-earthquake design in different regions. The SMCAR is now open to the public
105 on the web system of the 5th generation “Seismic ground motion parameter zonation maps” (GB18306, 2023), and has a geospatial database edition in addition to print and Joint Photographic Experts Group editions. This database integrates seismo-active faults in China and adjacent regions and is also known as CAFD (2015). After geospatial correlation by remote sensing images in the WGS84 coordinate system, its spatial accuracy was better than that of previous congeneric maps and data. The fault data included the fault attributes of the name, main character, and faulting age. A simplified version
110 is applied to construct a probabilistic seismic hazard model for Mainland China (Rong et al., 2020).

3 Latest version of China Active Faults Database

3.1 Active faults database compilation workflow

The CAFD (2022) presented in this paper, which is based on the most reliable results of the projects introduced in Section 1, is an updated version of the CAFD (2015). The compilation workflow of the database is illustrated in Fig. 1.
115 The data used to update the older version are obtained from project databases and research on active fault surveys, earthquake surface rupture investigations, and published literature in the past 20 years. 115 project databases, which have a scale of 1:250 000 or 1:50 000, are used to update the nationwide active fault database in China (Section 3.3). These data are obtained and produced under the same technological system based on well-established knowledge of active fault surveys (Section 3.2) and meet the technical demands of the Chinese mandatory standard (GB/T 36072-2018). Every project
120 database uses the same data schema and standard recommended by the China Earthquake Administration (GB/T 36072-2018; DB/T 53-2013; DB/T 65-2016; DB/T 81-2020; DB/T 82-2020; DB/T 83-2020). All parameter values of the fault data are calculated using the same systematic criteria and definitions (Section 3.5). As the data definition, schema, and acquisition method are the same, there is no information gap between these project databases. All data are processed using the same workflow. First, multiple-scale active fault data are extracted from different databases. Second, they are used to update the
125 geometric shapes and attributes of the corresponding fault data in a nationwide database. Finally, the updated database (2022) is translated into English, adjusted for deployment, and released online (Sections 3.4 and 3.6).

The CAFD (2022) is obtained from numerous surveys and research references. It reflects the current state of the integrated knowledge based on seismo-active fault surveys in China.



130

135

140

145

150

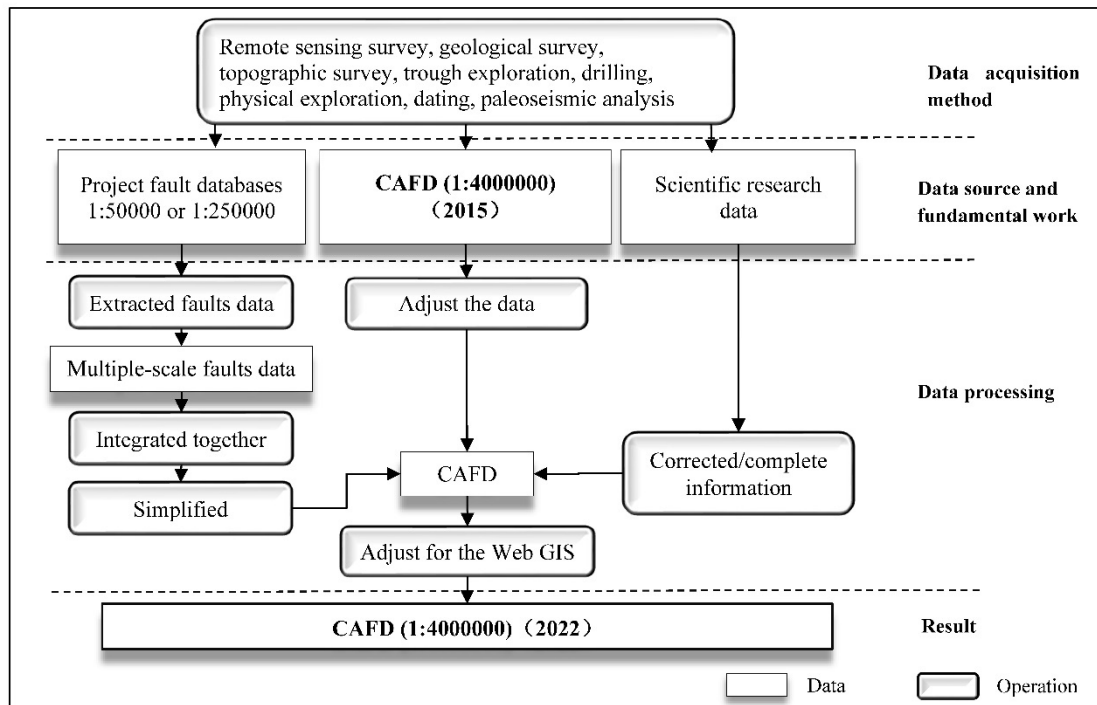


Figure 1: Workflow to construct the China Active Faults Database

3.2 Data acquisition and methods

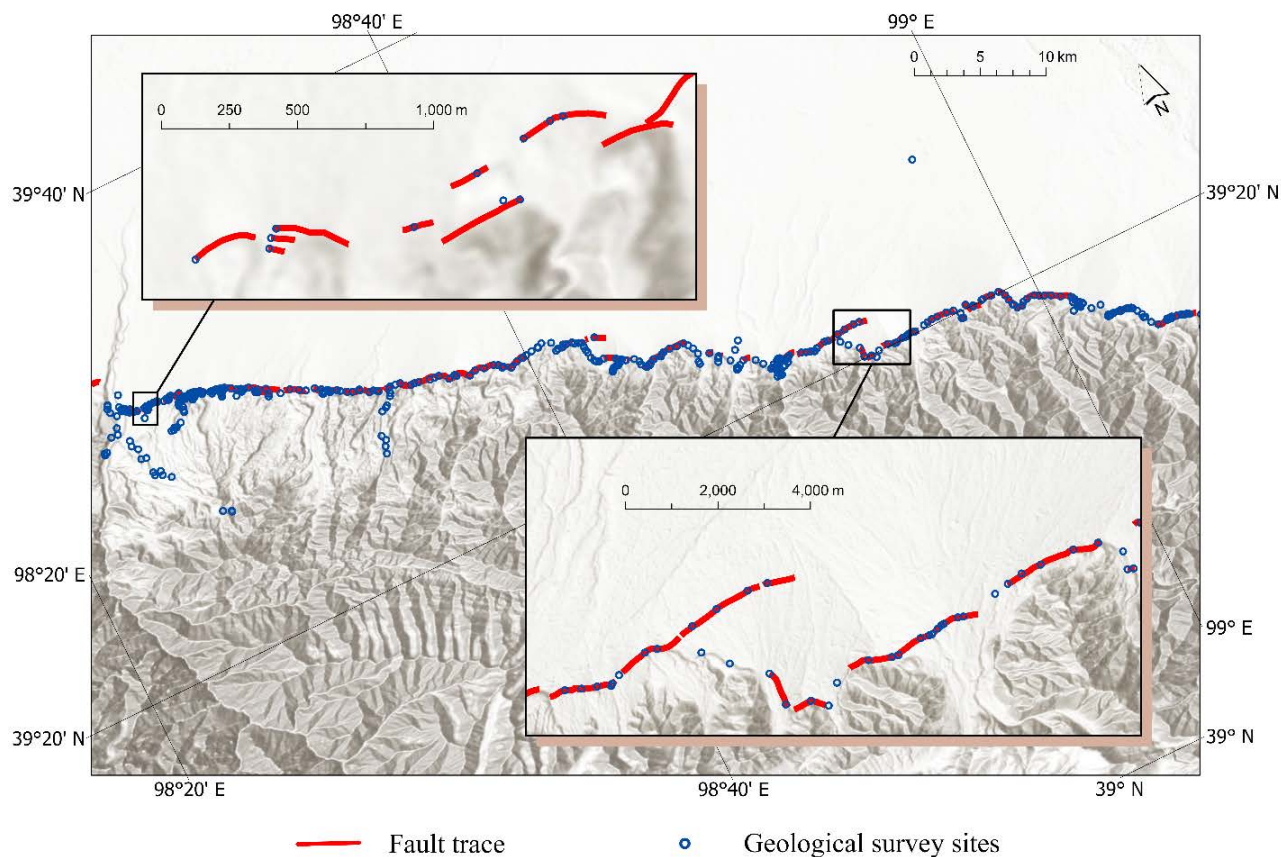
155 Location, geometric, and kinematic parameters of the faults stored in the nationwide database (1:4 000 000) (Xu et al., 2016) and survey project databases (1:250 000–1:50 000) are obtained through remote sensing data interpretation, geological field surveys, trenching, drilling, geophysical prospecting, dating, and paleo-seismic analyzing. However, the accuracies of nationwide and survey project databases differ from each other. The nationwide database (Xu et al., 2016) is based on previous studies. In earlier research, the positional precision of the exposed faults was restricted by funding and locator devices, and interpreted top breakpoints of the blind faults from low-resolution seismic petroleum exploration profiles restricted their positional precision. The fault survey project databases (1:250 000–1:50 000) are based on quantitative

160



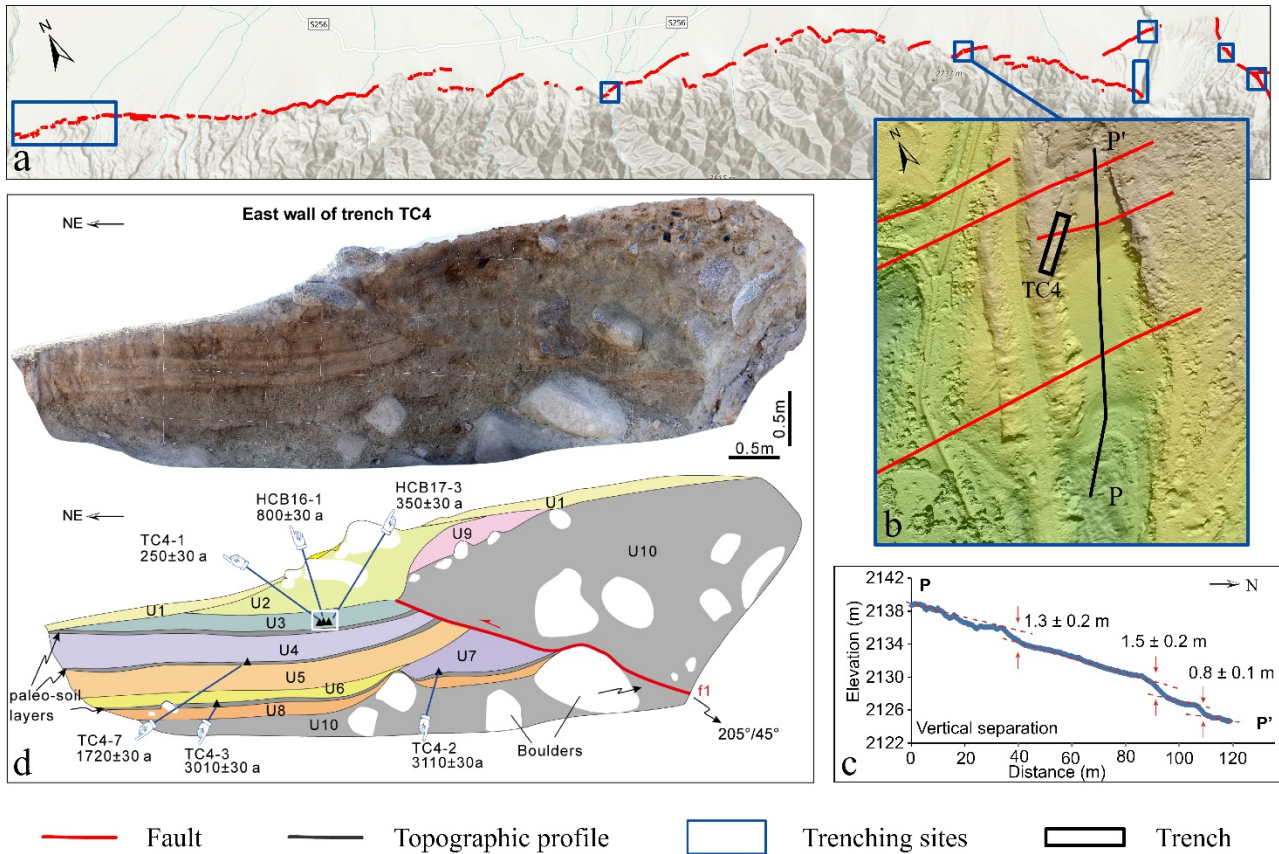
methods, that is, the exposed and blind fault survey methods, which guarantee better data quality and accuracy than the nationwide database (Xu et al., 2016).

For the exposed faults with surface traces, remote sensing and DEM (Digital Elevation Model) data are used first to map the
165 fault traces and create an initial distribution map of the active faults. Then, combined with the field surveys, the locations of
the faults in this initial map are verified, corrected, and completed. Finally, a systematic method that combines
geomorphological surveys, stratigraphic analyses of the geological cross sections, trench stratigraphic logs, sample dating
from terraces and trenches, and paleo-earthquake identification are used to obtain the latest faulting ages and kinematic
170 parameters of the mapped active faults (DB/T 53-2013; Chen et al., 2016; Sun et al., 2017; Shi et al., 2019, 2022; Guo et al.,
2021; Huang et al., 2021a), such as the Fodongmiao–Hongyazi Fault, which is mapped at a scale of 1:50 000 (Yang et al.,
2018a, 2018b, 2020; Huang et al., 2021a, 2021b). Firstly, remote sensing images with meter-level resolution and DEMs with
horizontal and vertical resolutions of > 5 m are used to mark surface deformations or offset landforms (fault scarps,
dislocated gullies, fault valleys, pull-apart basins, Pressure ridges, terraces, alluvial or fluvial fans and so on) and plan
geological survey sites, lines, and areas. Following these marks and positions, the fault could be traced along the fault strike,
175 and the coordinates of the exposed fault site are precisely recorded by using Global Navigation Satellite System. The average
interval of coordinate-recording sites is 500–2 000 m, but if the surveyor could get to the spot an interval of 500 m is
required (Fig. 2; DB/T 53-2013). The density of the recorded sites controls the geometric accuracy of the fault data to ensure
the horizontal location error less than 15 m. If the surface deformations or offset landforms disappear in some areas, the
approximate fault location should be taken from the original interpretation of the high-resolution remote sensing images and
180 DEM data. Subsequently, the next exposed fault segment is searched by traveling across the region in a “Z” route. When the
next fault segment is identified again, the fault should be traced along its strike. After these steps, the geometry of the fault
trace is finally confirmed on the map. Once the fault trace is ascertained, the fault is separated into segments based on the
mapped geometry. Along the key segments, typical offset landforms should be selected for further geomorphic and
topographic measurements (Fig. 3a & c). In every independent segment, dislocated strata, samples and trenches are
185 accurately located, and the number of paleo-earthquake events are revealed in the trenches (Fig. 3b & d). The ages of
dislocated strata are measured by using dating methods. Common dating methods include radiocarbon (^{14}C), cosmogenic
nuclides (^{10}Be), and luminescence techniques. They are used to identify whether or not a fault is active, to calculate its slip
rate during a certain time period, to determine when a paleo-earthquake occurred, paleo-earthquake recurrence interval and
the elapse time of the last earthquake of the corresponding fault segment.



190

Figure 2: Survey sites for mapping of the Fodongmiao–Hongyazi Fault. The average interval of coordinate-recording sites ranges 500–2 000 m. The fault belongs to the Qilianshan thrust fault zone at the northeastern margin of the Tibetan Plateau.



195 **Figure 3:** Key fault segment surveying example from the Fodongmiao–Hongyazi Fault (red line). (a) Distribution of the key fault segments in which geomorphic measuring, trenching, sample collecting, and paleo-earthquake trenching sites are marked by dark blue rectangles; (b) Locations of trench TC4 and topographic profile P-P' are represented by black rectangle and black line, respectively; (c) Topographic profile (P-P') showing fault offsets (adapted from Huang et al., 2021b); (d) Interpretation of the east wall of trench TC4 in detail (adapted from Huang et al., 2021b).

200

The approximate location of the blind fault was inferred first from the collected previous petroleum exploration profiles, historical earthquakes, and published references. Secondly, a comprehensive multi-level exploration method is applied to determine its exact near-surface location and the position of the uppermost displaced point of the major blind fault. Then by using drilling and dating techniques to obtain samples of the displaced and un-displaced strata and their dated chronological ages to identify its late Quaternary activity. This method consists of multi-level seismic exploration, joint drilling to construct a fault-across geologic section, trenching, and other technologies to detect the blind active faults from deep to shallow or even directly to the surface. In this study, the blind Yinchuan active fault is used as an example (Fig. 4; Chai et al. 2006, 2011; Liu et al. 2008) to describe the quantitative technical demands written into the Chinese mandatory standard in 2018 (GB/T 36072-2018). Firstly, the seismic petroleum exploration profiles are used to reveal the approximate location of the target fault at a depth of hundreds of meters and the bottom of the Quaternary, marked by the shallowest continuous

205

210



seismic reflection layer. Based on this information, a set of shallow seismic exploration profiles (in an interval of ≤ 2.5 km) is set up on the approximate ground to detect the depth of the uppermost point of the target fault. Secondly, two boreholes are drilled on both sides of the detected target fault to preliminarily verify the existence of the target faults (Fig. 5). Then, the exploration of the joint drilling geologic section is planned based on above preliminary verification. During this exploration phase, the borehole number is gradually increased on both sides of the target fault to locate the depth of the uppermost points of the faults (Fig. 6; Chai et al., 2006; Lei et al., 2008; Wang et al., 2016). It requires at least 3 boreholes on each fault wall, with an interval of 5–45 m. The distance between the two boreholes on both side of the target fault should be less than 10 m. Also at least one borehole is required to penetrate the bottom of the Upper Pleistocene on each side, and the final depth of other boreholes is needed to be 10 m beneath the uppermost points determined by the shallow seismic exploration (GB/T 18306-2018). The exact location and faulting age of the target blind fault could be identified by strategic analysis and sample dating of the borehole cores. If the depth of the uppermost points determined by the joint drillings is less than 10 m deep from the ground, more information on the blind fault geometry and paleo-earthquakes could be revealed by trenching. The mapped blind fault trace is a line of vertically projected the uppermost points on the ground, which are obtained by using the comprehensive multi-level exploration method.

225

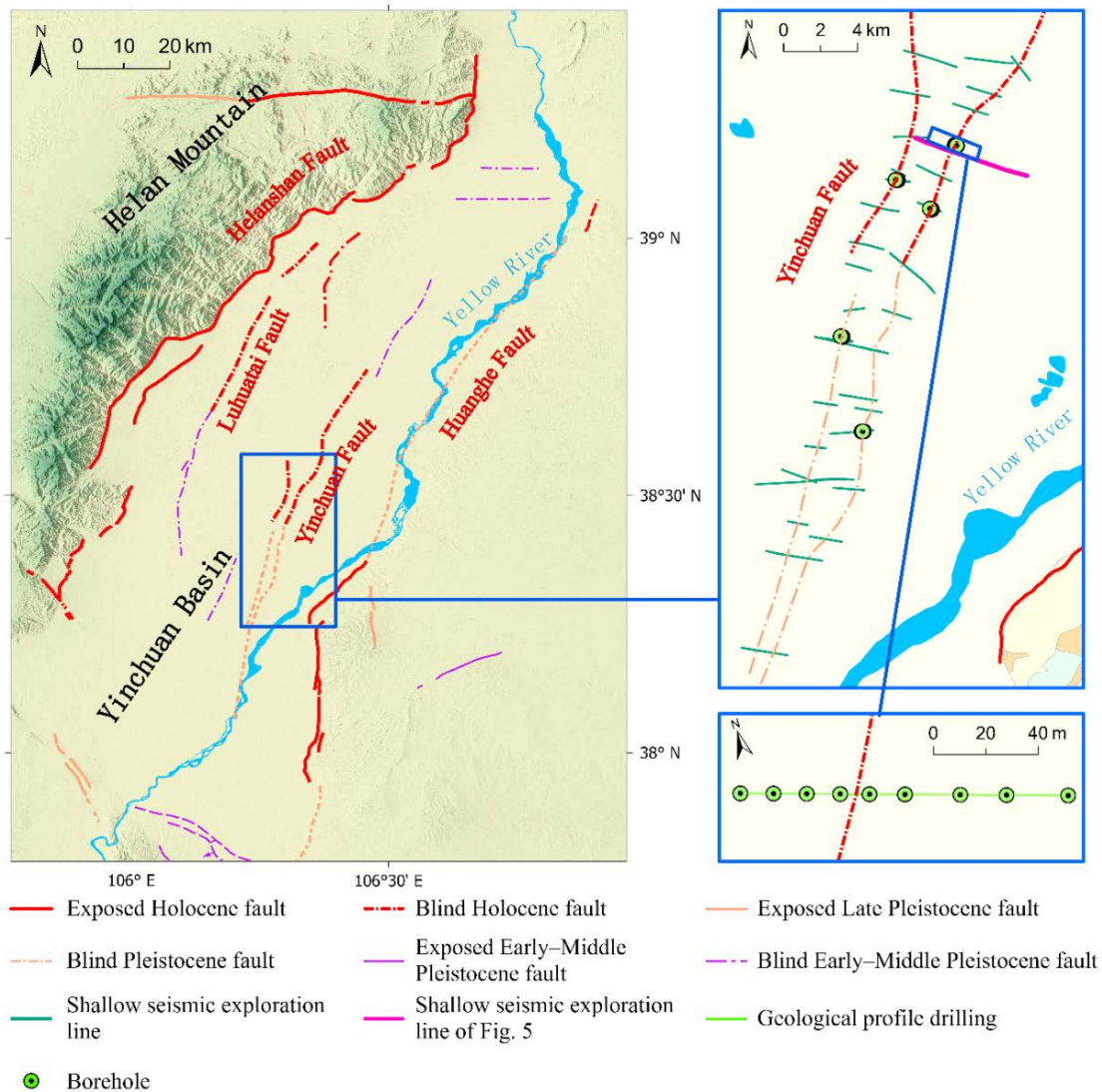
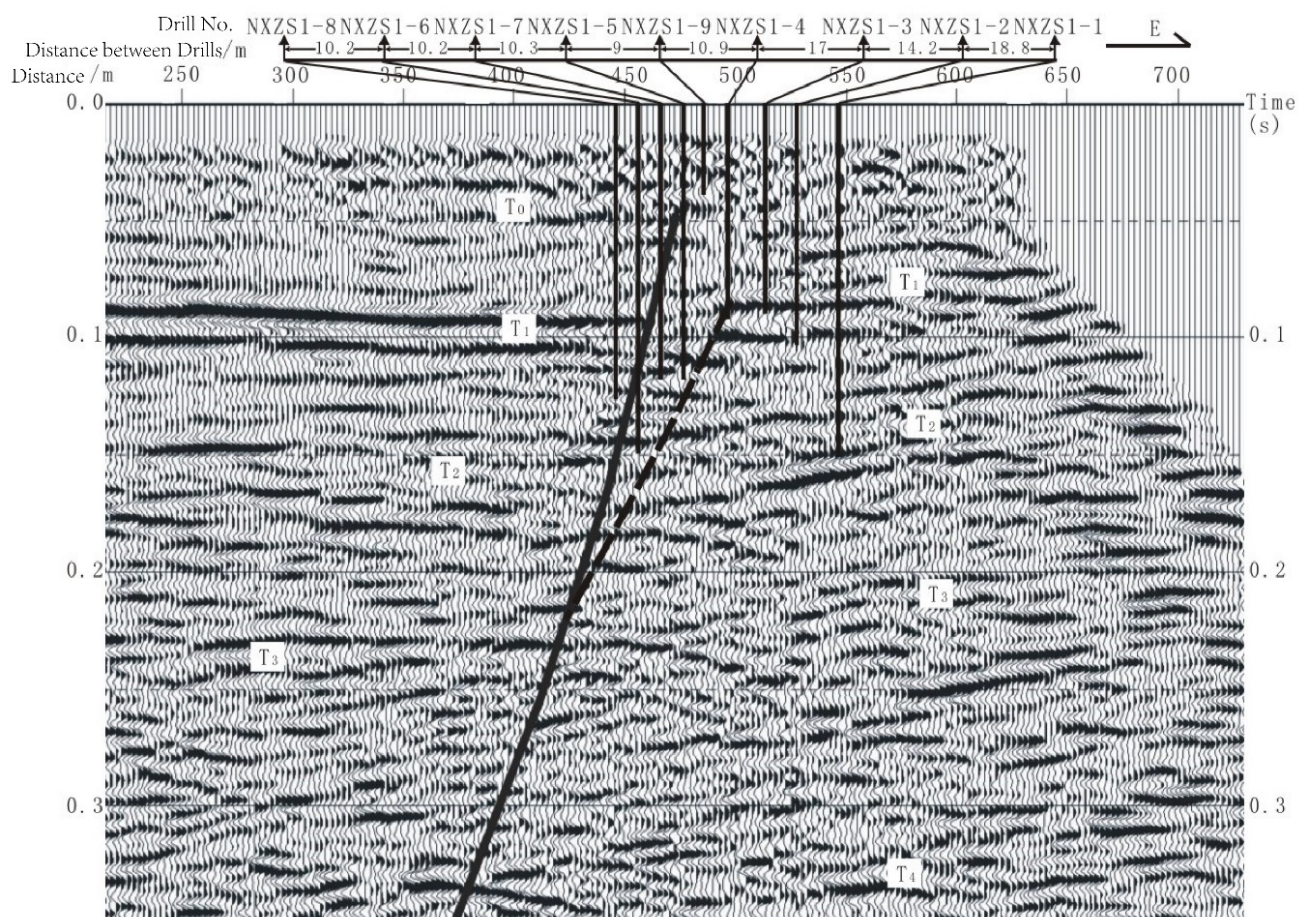


Figure 4: Map of the blind Yinchuan Fault in the Yinchuan Basin located in the northern portion of the North-South seismic zone in China.



230 **Figure 5: Approximate locations of the detected target fault and boreholes along a seismic exploration profile (adapted from Chai et al., 2011, Xu et al., 2015).**

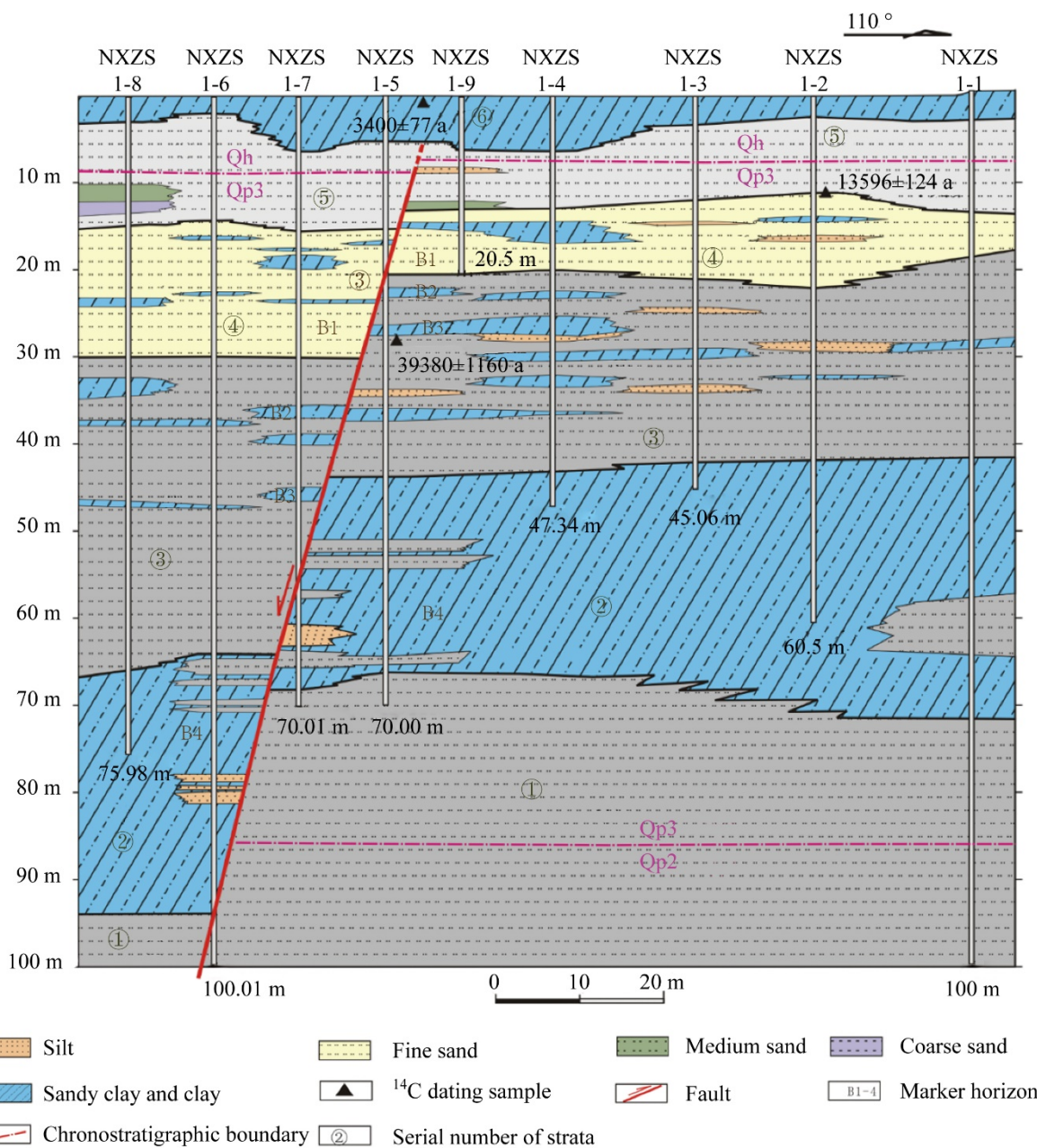


Figure 6: Joint Drilling geological cross section at Xinqushao Village in the Yinchuan Basin (adapted from Lei et al., 2008; Chai et al., 2011).



3.3 Data sources and fundamental works

The CAFD (2022) was updated by integrating new data from the projects of active fault surveying in urban regions, seismo-active fault mapping at a scale of 1:50 000 in the north China and North-South seismic zone, and seismic risk assessing of the active faults in the key earthquake surveillance and prevention areas, and other scientific researches (Fig. 7). These projects are introduced in detail below:

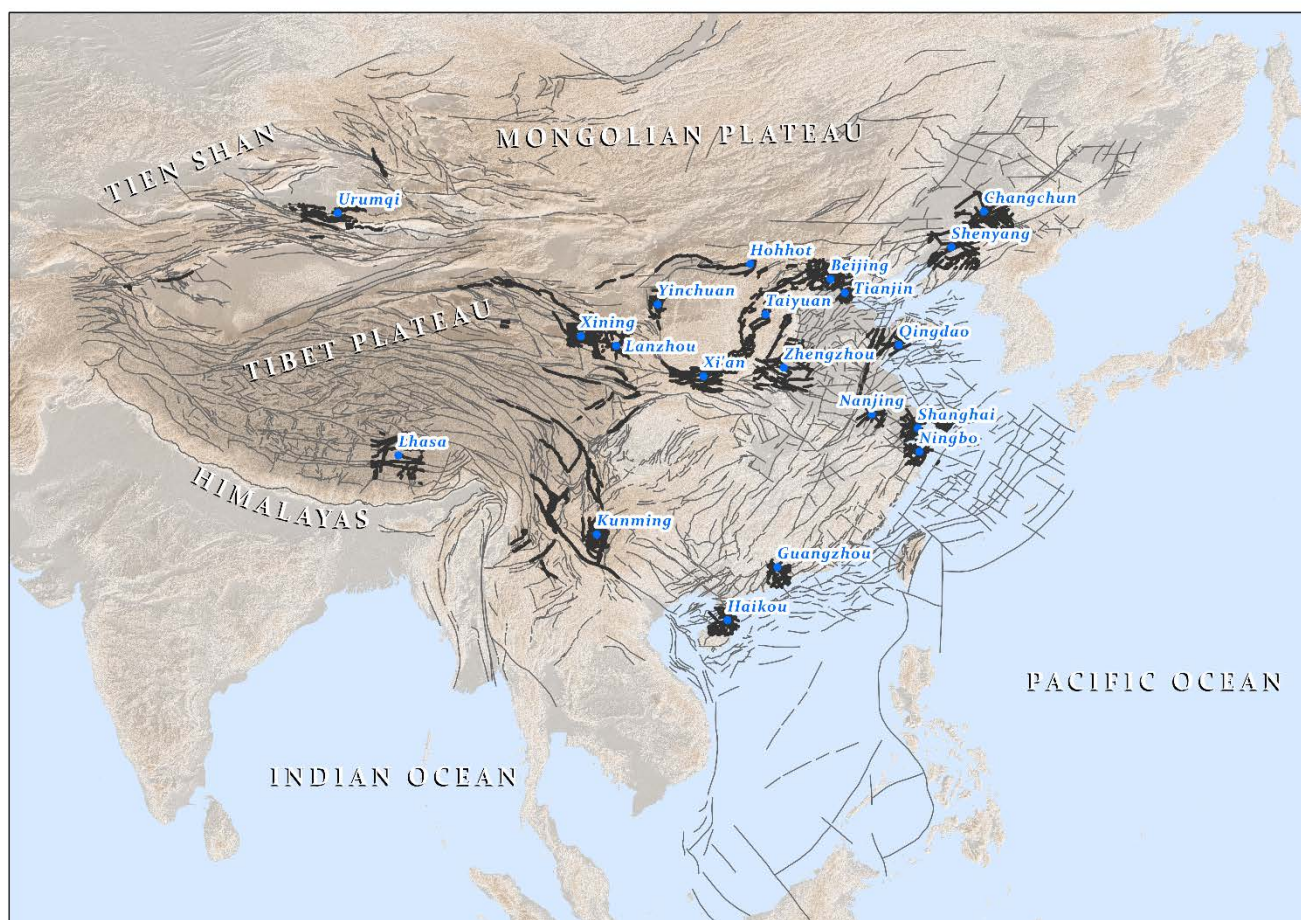
The projects of active fault surveying and seismic risk assessing focuses on locating the blind or exposed seismo-active faults and assessing the earthquake risk in large- and medium-sized cities and in the key earthquake surveillance and prevention areas, while the project of active fault mapping on locating the exposed seismo-active faults in detail for land-use planning and utilization (Xu et al., 2015; Zhu et al., 2005; Chai et al., 2011; Liang et al., 2013; Shen et al., 2016; Hou et al., 2012; Chen et al., 2013; Yang et al., 2010). The fundamental works of these projects mainly include five parts: (1) initially identifying fault activity, (2) detecting deep structures of the fault in the crust, (3) assessing earthquake risk possibility for the identified major faults to judge an seismo-active faults, (4) locating the detailed geometry of the major seismo-active faults, and (5) evaluation of earthquake hazards on the seismo-active faults. Achievements of these projects include maps, which demonstrate regional distribution of the active faults at a scale 1:250 000 and detailed faults traces of a single active fault at scale 1:50 000, exploration reports, project databases, and information systems (Xu et al., 2015). All of those data obtained from the fundamental works and also the project achievements are carefully reviewed by three to eight experts from a professional panel. Therefore, the data results were credible. These projects have been carried out in ~100 cities, including 26 provincial capitals and municipalities, until March 2020. Twenty urban active fault survey project databases, which were conducted from 2002 to 2009 in Beijing, Tianjin, Shanghai, Nanjing, Ningbo, Zhengzhou, Qingdao, Hohhot, Taiyuan, Xi'an, Yinchuan, Lanzhou, Xining, Lhasa, Kunming, Urumqi, Haikou, Guangzhou, Changchun, and Shenyang (Fig. 7), are earliest fault data published and released to the public (Xu et al., 2015), and are also used to update the nationwide active fault database.

Active fault survey and mapping projects on scale 1: 50 000 and 1:250 000 are funded by China Earthquake Administration. The goal is to obtain the exact location, spatial distribution, geometric and kinematic parameters, activity age, slip rate, paleo-earthquake events and their recurrence intervals and the elapse time of the last surface-rupturing event on the faults. These projects followed the procedure introduced in Section 3.2 and meet the quantitative requirements of mandatory and recommended standards (GB/T 36072-2018; DB/T 53-2013; DB/T 65-2016; DB/T 81-2020; DB/T 82-2020; DB/T 83-2020). A professional panel reviewed the field data and mapping results to guarantee data quality. In this study, ~140 mapped faults (Fig. 7) in the North China, the North-South seismic zone and the Tianshan region are selected to update the nationwide active fault database.

The focus of scientific research projects has been placed on answering specific scientific questions about active faults and earthquakes. In those projects, seismo-tectonics and seismo-genesis at some sites or in some regions are studied based on the fault's geometric and kinematic features. The results are credible and provide parameters such as the reliable slip rates, plaeo-



270 earthquake sequences, potential magnitude of the future earthquakes, coseismic slips and their distribution along the strike of
a seismogenic active fault. To update the nationwide active fault database in this study, data from the 2008 M 8.0 Wenchuan
Earthquake investigation (Xu et al., 2008a, 2008b, 2009a, 2009b; Chen et al., 2009), 2014 M 6.5 Ludian Earthquake
investigation (Xu et al., 2014a, 2014b), Xia-Dian Fault survey (Xu et al., 2000; He et al., 2013), and research on the Tanlu
Fault (Shu et al., 2016, 2020; Li et al., 2019) were used (Fig. 7).



— fault data used to update the nationwide database — fault data ● 20 large cities for which data were updated

275 **Figure 7: Sketch map of updated fault data in China.**

3.4 Data processing

280 The CAFD (2015), project databases of active fault surveys and mappings in different regions and the scientific research
data have been established. The data are complex, with multiple scales and accuracies, and the total data size is large. As
introduced in Section 1, the databases of active fault surveys and mappings include 115 sub-databases with a total size of ~7



Terabytes of data. All data are supervised and reviewed by professional panels to ensure them all highly accurate and reliable. For the primary purpose of introducing the newest integrated achievements in this study, the reliability of fault data are not individually described. To integrate those large datasets into a unified database with the same data criteria and schema, we first integrated those project-databases constructed in regional scale and then update the national-scale CAFD (Fig. 1). Major
285 updates of the 1:4 000 000 nationwide database include the activity ages and locations of the late Pleistocene and Holocene faults.

The project databases of active fault surveys and seismo-active fault mappings are constructed by using the same criteria. They have the same data schema and use unified, well-established acquisition methods. Therefore, the fault data from these two types of databases can be processed using the same procedures, with a small workload for data cleaning and mining. The
290 first step involves extracting multi-scale fault data from the 115 project databases. The second step is to integrate them. These projects are systematically planned so that, theoretically, fault data with the same scale do not overlap. If the same region contains more than one fault trace, only the largest-scale data are used for integration. As the scales of the new well-mapped fault traces are equal to or even larger than 1:250 000, they are too complex to be integrated into 1:4 000 000-scale data. Therefore, the third step is to simplify the fault traces. In large-scale fault data, a fault is generally segmented for
295 detailed investigation; hence contiguous segments may have different activity ages. When integrated into the national scale fault data, two or even more small contiguous segments may be merged into one. Under this condition, the activity age of the merged fault trace is the same as the latest of the merged segments. For example, the blind Yinchuan fault (1:250 000) is divided into the Holocene north segment (Fig. 4a, red dotted line in the blue rectangle) and late Pleistocene south segment (Fig. 4a, orange dotted line in the blue rectangle). The total length of those two segments is 80 km, which is only 2 cm on a
300 1:4 000 000 scale map. Therefore, the two segments are merged into a Holocene one.

Scientific researches have mainly focused on one segment or a limited number of surveying sites for one fault. Those data are used to supplement the CAFD (2022), to complete and correct the national-scale fault data using a similar method. The CAFD (2015) was based on the same data definition and acquisition methods previously described, but its data schema slightly differs from the project databases of the fault surveys and mappings with respect to field names and domain values.
305 Considering that the CAFD (2015) has fewer fault traces than the project databases, we adjust the CAFD schema to fit the project databases. Subsequently, the processed data introduced in the previous two paragraphs are smoothly integrated into the CAFD (2022). The CAFD (2022) is adjusted for deployment in the Web-GIS system before being published in the last step.

3.5 Data descriptor

310 The active fault database is translated into English before being deployed in the system and released so scientists and engineers could use it worldwide. Its fields include the fault zone name, fault name, fault segment name, kinematic features, and activity age (Table A1).



The fault data are graded based on size and characteristics using the fields of fault zone name, fault name, and fault segment name. A fault zone is a large fault system such as the Tanlu and Longmenshan fault systems. A single-fault system consists of several faults. A single fault is divided into multiple segments. Each segment has specific and different geometric and kinematic characteristics and is a basic studied unit of a fault. Each fault line data point belongs to one fault segment. Not all faults belong to a fault system.

Only some important active fault line data belonging to a fault system in block boundary zone have a “fault zone name”. Some highly studied faults are divided into segments and the corresponding fault line data have “fault segment names.” Because of the complications and massive number of faults in China, rating and naming must be continued.

The field named “feature” stores the motion type and visibility from the fault on ground. Based on the relative movement of the two walls, the faults were classified as normal, reverse, strike-slip or oblique faults. Oblique faults consist of left- and right-oblique slip faults. Active faults are also divided into exposed, buried, and inferred faults.

The active fault database is aimed at earthquake hazard reduction and focuses on the latest activity during the Quaternary. Therefore, faults are classified as the Holocene, late Pleistocene, middle–early Pleistocene and pre-Quaternary faults, denoted by the field “Age” (GB/T 36072-2018). The Holocene faults are those with active evidence from the Holocene or the past 12 000 years. For the late Pleistocene faults, active evidence exists in the late Pleistocene but not in the Holocene. The middle–early Pleistocene faults are those with the latest active evidence in the middle or early Pleistocene. For pre-Quaternary faults, active evidence is not available in the Quaternary. Major active evidence is based on the latest dislocated stratum. This method is introduced in Section 3.2.

3.6 Quality discussion

The CAFD (2022) collects the maximum amount of reliable data relative to earthquakes with the primary objective of effectively reducing earthquake hazards by determining earthquake sources and carrying out active tectonic zonation. It performs well in terms of quantity and quality. The spatial correlation between faults and earthquakes with magnitudes greater than 6.5 is high. The amount of fault data is large. The database contains ~7 000 fault traces, among which 1 606 faults are named.

Active fault surveys in China are difficult because the country is located in the intersection region of the Circum-Pacific and Eurasian seismic zones, resulting in complex continental tectonics, widely distributed active faults, strong neotectonics and earthquake activities, and inaccessible landforms. The extent of seismo-genic fault research varies from region to region in China. For some faults with low research extent, their geometric and kinematic parameters remain unknown or imprecise. In the periphery and interior of the Tibetan Plateau, which has been formed during the colliding between the Indian and Eurasian Plates, there exist meg-strike-slip fault systems, such as the Altyn Tagh, east Kunlun and Xianshuihe Faults, the thrust fault systems, e. g. the Himalayan frontal, Hexi Corridor and Longmenshan thrusts, and the North-South striking normal faults in the western Plateau. The thrusts and strike-slip fault have also been developed at the northern and southern piedmonts and in its interior. In some regions in the Tianshan and Tibetan Plateau due to the high altitude and snow-capped,



it is difficult to carry out research work and obtain accurate fault data. There exist numerous oblique normal faults around the Ordos Block and strike-slip faults, such as the Tanlu fault in the eastern China. Those faults are located in the regions with dense urban construction and populations or thick quaternary deposits. Therefore, it is difficult to find out those fault traces on the ground and locate the blind faults underground. Besides, the spatial relationship and geometrical link of some faults, such as some segments of the Tanlu fault in the eastern China and some E-W trending faults in the Tibetan Plateau, also remain unclear.

Thus, the vector lines of such faults directly cross each other without expressing a geometrical link. In addition, research on marine and maritime island faults has been limited by surveying technology.

As the Active Fault Database in China is based on 1:4 000 000 data and was updated by 1:250 000–1:50 000 data, the total coordinate accuracy is similar to the 1:1 000 000 map in which 1 mm is equal to 1 km in the real world and represents the width of the fault line symbol. The data precision is partially better than that of the 1:1 000 000 map because the reference is on a larger scale.

Based on the discussion above, the CAFD (2022) is based on the latest research on active faults and fault data integration. More investigations of active tectonics and fault systems should be carried out in China, and the nationwide database should be updated in the future.

3.7 Application

The CAFD (2022) and its previous versions have been widely used by the Chinese government, research institutions, and associated companies. The National Geomatics Center of China and the China Petroleum & Chemical Corporation take those data as reference data to analyze the seismotectonic environment for their information management systems. The national-scale Active Faults Database is the basic reference for compiling seismotectonic maps on a regional or national scale. Examples include the seismotectonic map of the Ordos block and its boundary zones (1:500 000; National Research and Development Program of China; No. 2017YFC150100), digital seismotectonic map of the northeastern seismic zone in China (1:1 000 000; a Spark Plan project funded by the China Earthquake Administration; No. XH18015), seismotectonic map of the Shanxi Province and its adjacent regions (1:500 000; a public service map produced by the Shanxi Earthquake Agency), and seismotectonic map of China (1:1 000 000; first comprehensive natural hazard risk investigation in China). They are also used in earthquake emergency response services, monitoring services, forecasting services and earthquake disaster preventions supervised by the China Earthquake Administration. The database has been delivered to the earthquake response departments of the China Earthquake Networks Center for emergency actions since 2018. In 2018, it was also delivered to the working research group of the post-earthquake prediction technology system, a key project in the earthquake monitoring and forecasting from China Earthquake Administration (Project No. 18440680117). In 2019, this database was transferred to the China Earthquake Disaster Prevention Center to establish the Data Center for Seismic Active Fault Surveys. The Institute of Geology, China Earthquake Administration (IG, CEA), has also produced the seismotectonic maps during earthquake emergencies based on the database (Wu et al., 2021). As the system discussed in this study was released online, a



commercial app (GeoQuater) became available that uses the WFS service of this database as a thematic map. The WFS
 380 service is stable on the application.

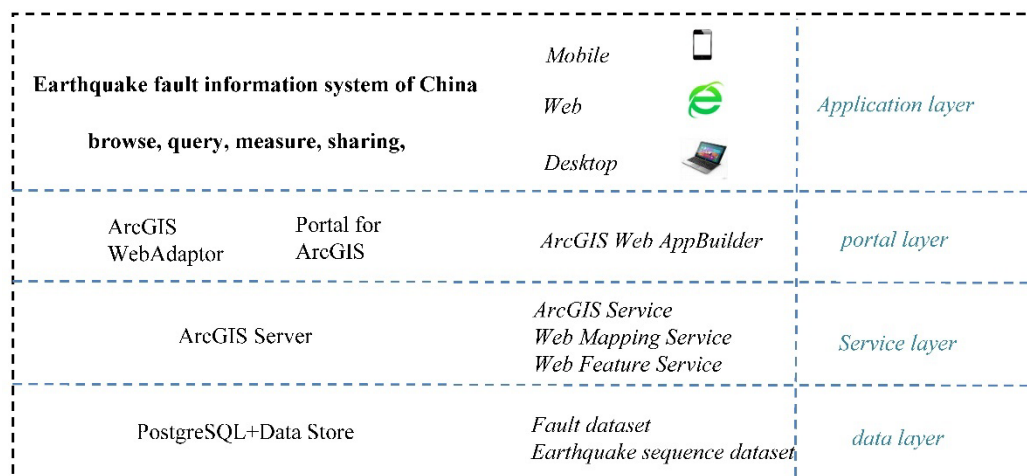
4 System introduction

4.1 System performance and architecture

The China Earthquake and Fault Information System (CEFIS(V1), 2021), which has been launched online and updated since
 2019, provides web services for inquiring about earthquakes and active faults in China and adjacent regions. The CAFD
 385 (2015) has been released in the system. In 2021, the system was updated again by simplifying the interface, adding the
 English fields, earthquake base map, layer addition and system sharing function. A simplified case of a regional active fault
 survey map (Wu et al., 2022), introduced in Sec 3.3, is also open to public as a map service in the additional layer list. This
 section introduces the architecture of the URL's current version (CEFIS (V2), 2023).

The system is constructed on ArcGIS Enterprise platform 10.6 using ArcGIS Web AppBuilder in the B/S mode and is
 390 separated into four layers (Fig. 8) namely data, service, portal, and application layers.

The data layer deploys the PostgreSQL database to store active fault and earthquake data. PostgreSQL is a free open-source
 object-relational database system that can be connected to an ArcGIS Server deployed in the service layer. The ArcGIS
 Server can publish data in the form of map and feature services, which can be conveniently called web applications. The
 ArcGIS Portal and ArcGIS Web Adaptor are deployed in the portal layer to provide WMS and WFS services and manage
 395 user access. The ArcGIS Portal provides intuitive what-you-see-is-what-you-get applications such as AppBuilder with ready-
 to-use widgets. These applications are used to construct a map and three-dimensional scene applications on the web. The
 system in this study is also constructed using ArcGIS Web AppBuilder. Supported by these technologies, the CAFD can be
 accessed on various platforms through desktop software, smartphones, and online sites.



400 **Figure 8: System architecture diagram.**



4.2 Earthquake sequence data

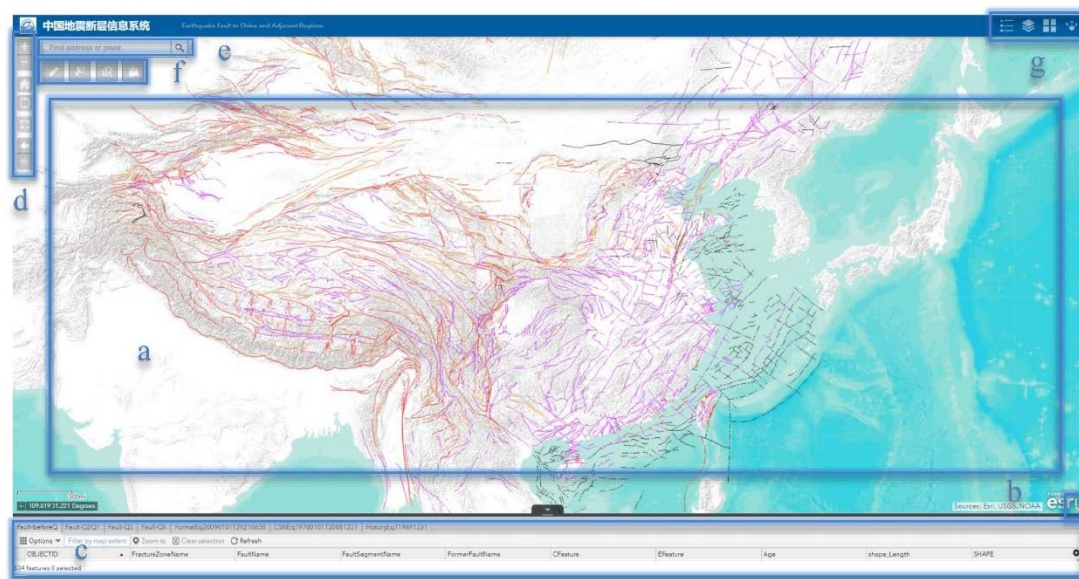
The system uses earthquakes ($M > 5.0$) as a background to show earthquake activity on and around faults. The earthquake catalog from the National Earthquake Data Center (NEDC) is converted into geographic vector data and deployed in the system (Earthquake sequence data from NEDC, 2023). It contains historical and instrumental-recording earthquakes that
405 occurred before June 2021. The system contains three earthquake layers. Those correspond to the three datasets downloaded from the NEDC. The NEDC provide three datasets based on the following time periods: a historic earthquake catalog (before
~1969.12.31.; Table A4), the earthquake catalog of the China Earthquake Networks (CEN; 1970.1.1.-2008.12.31.; Table A3), and the official earthquake catalog from the CEN (2009.1.1.-2021.6.30.; Table A2). The historic earthquake catalog compiled by Gu (1983) includes destructive earthquakes ($M \geq 5.0$) that occurred from 1831 BC to 1969 AD. The CEN
410 earthquake catalog consists of data from 88 National seismograph network stations (digital), regional someone-on-duty network stations (digital), and simulated network stations. The official earthquake catalog is from CEN, which is obtained from a nationwide earthquake monitoring station networks consisting of national and regional (31) station networks after January 1, 2009.

4.3 System using

415 4.3.1 System interface and function

The system is a Web Map application that displays and queries the Active Faults Database of China and its adjacent regions. It is publicly available worldwide. The system interface consists of seven parts (Fig. 9): (a) web map, (b) eagle-eye map, (c) attribute table, (d) browsing tools, (e) address geolocation tool, and (f & g) system tools.

The language of the system interface is based on the browser's default language. The data field values are in both of English
420 and Simplified Chinese in the attribute table and Query dialogue. Thus, the system can be used by both English and Chinese users.



425 **Figure 9: System interface. (a) Web map displaying only fault traces in full extent view; when zoomed into the regional-scale, earthquake epicenters will appear on the map. (b) Accordion overview map. (c) Accordion attribute table. (d) Navigation toolbar; the tools from top to bottom are zoom in, zoom out, default extent, zoom to the current position, full extent, previous view, and next view. (e) Address geolocation tool. System tools: (f) measurement, selection, inquiry, and layer addition (from left to right) and (g) legend, layer controller, base maps, and sharing (from left to right).**

4.3.2 Data query and export

430 The system provides four methods for querying fault information: (1) The menu of the attribute table window (Fig. 9a) provides a “filter” tool to query faults with certain conditions (Fig. 10a); (2) the second tool is a spatial selection tool (Fig. 9f) for fault and earthquake data (Fig. 10c); (3) the third tool allows fault queries by feature, activity age, or name under specific spatial conditions (Figs. 10b and 9f); (4) the address geolocation tool (Fig. 9e) can be used to zoom the map into a specific region and export the faults in that region (Fig. 10d). The system can export the query results using diverse methods (Fig. 10).

435

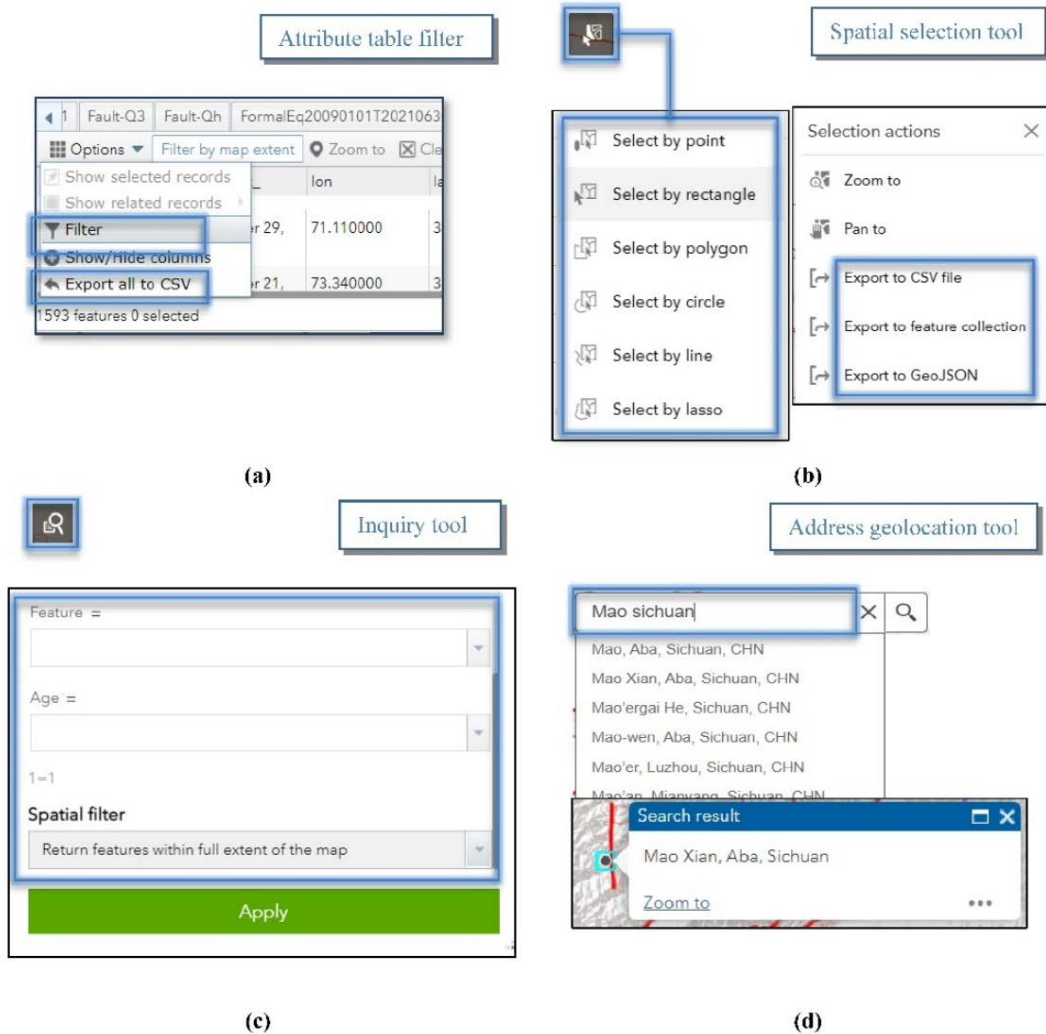


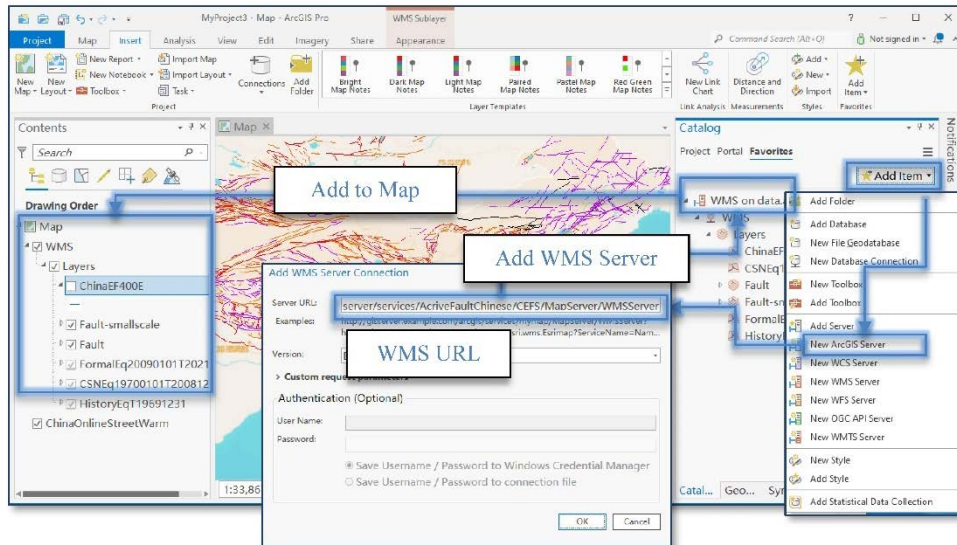
Figure 10: Data query and export tools: (a) attribute table filter, (b) spatial selection tool, (c) inquiry tool, and (d) address geolocation tool (translated by Google Chrome).

4.4 How to use the data service

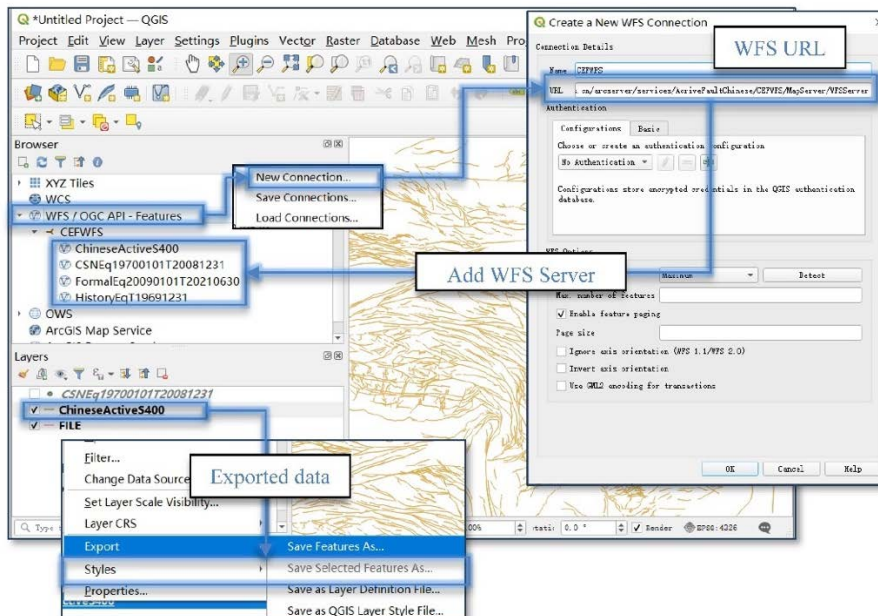
440 The system publishes the Open Geospatial Consortium (OGC) WFS and WMS (Table 6) of the active fault database of
China. The OGC WFS and WMS are dynamic services that provide dynamic maps on the web, following the specifications
of the OGC. These services allow web maps to access diverse platforms and clients openly and authentically. Available
operations of the WMS in the system in this study are GetCapabilities, GetLegendGraphic, GetSchemaExtension,
GetFeatureInfo, and GetMapGetStyles. Compared with WMS, WFS provides greater data access, benefiting from its ability
445 to insert, update, delete, retrieve, and discover geographic elements over HTTP in a distributed environment. Available WFS
operations are GetCapabilities, DescribeFeatureType, GetPropertyValue, GetFeature, GetGmlObject, ListStoredQueries, and



DescribeStoredQueries. In other words, data can be browsed, queried, analyzed, and downloaded from the system, but not revised. Fault layers can also be added to GIS software for the analysis through WMS and WFS such as ArcGIS Pro and QGIS (Fig. 11).



(a)



(b)

450 Figure 11: (a) How to add WMS Server in ArcGIS Pro. (b) How to add WFS Server in QGIS and export data.



5 Conclusions

The CAFD (2022) is integrated with the national-scale fault database and the latest decadal regional-scale fault survey data and represents the most complete nationwide seismo-active fault data in China. The database and its previous versions have been widely applied in the government departments, research institutes, and commercial companies. China is situated in the intersection between the Circum-Pacific and Eurasian seismic zones with numerous complex continental tectonics, active faults and earthquake activity. However, it is difficult to survey or locate active faults in some regions due to inaccessible landforms and anthropogenic activities. Active faults should be considered for earthquake prevention and mitigation. Therefore, the database will be gradually updated in the future based on future references, and a later version may be released on the system if it is finished.

The first version of the web system (CEFIS (V1), 2021) has operated well for nearly 2 years and its second version (CEFIS (V2), 2023) was released in 2021 and has also been operating well. This study introduces its architecture, interface, function, and usage to provide a platform to query and analyze the integrated active faults database in China, which stores the location, latest activity age, and geometric and kinematic characteristics of the faults. Although the interface environment is in the Chinese language, English-speaking users can also use the system introduced in Section 4.3.

Data and services are openly shared worldwide via the web system. The data can be downloaded from browser or GIS software. A third-party application can link to and use the WMS and WFS services (CAFD WMS, 2023; CAFD WFS, 2023). Users can get help from the ArcGIS online document. Section 4.4 lists the available operations of the services.

6 Data availability

The CAFD and web system is accessible at CEFS (V2) under the DOI:
<https://doi.org/10.12031/activefault.china.400.2022.db> (Xu, 2022). The WMS (CAFD WMS, 2023) and WFS (CAFD WFS, 2023) services of the active fault are accessible online. The data are downloadable through diverse platforms and clients as introduced in Sections 4.3.2 and 4.4. The Earthquake catalogs are downloaded from the Data Sharing Infrastructure of the National Earthquake Data Center (<http://data.earthquake.cn>)

475

480



7 Appendix A

Table A1: Attributes of fault data.

Field name	Description
FractureZoneName_Ch	(in simplified Chinese) Fracture zone name. Only some
FractureZoneName_En	(in English) Fracture zone name.
FaultName_Ch	(in simplified Chinese) Fault name.
FaultName_En	(in English) Fault name.
FaultSegmentName_Ch	(in simplified Chinese) Fault segment name.
FaultSegmentName_En	(in English) Fault segment name.
FormerFaultName	(in simplified Chinese) Former name of fault.
Feature_Ch	(in simplified Chinese) Kinetic property and detectability of the fault segment.
Feature_En	(in English) Kinetic property and detectability of the fault segment.
Age	(in English abbreviations) The active age of the fault segment.

485

Table A2: Attributes of FormalEq20090101T20210630.

Field Name	Description
Date	The origin date and origin time of the earthquake (GMT +8).
lon	Epicentral longitude of the earthquake.
lat	Epicentral latitude of the earthquake.
dep_km_	Focal depth of the earthquake in km.
magnitudet	Magnitude type.
magnitude	Magnitude.

Table A3: Attributes of CSNEq19700101T20081231.

Field Name	Description
time_gmt_	The origin date and origin time of the earthquake (GMT).
lon	Epicentral longitude of the earthquake.
lat	Epicentral latitude of the earthquake.
dep_km_	Focal depth of the earthquake in km.
ms	Surface wave magnitude.
ms7	Surface wave magnitude computed from records of the Chinese-made long-period seismograph of type 763 (Cheng et al., 2017).
ml	Local magnitude.
mb	Body wave magnitude measured by short-period body wave recording (mb).
mb_1	Body wave magnitude measured by medium-period body wave recording (mB).

490 **Table A4: Attributes of HistoryEqT19691231.**

Field	Description
-------	-------------



Name	
time_beiji	The origin date and origin time of the earthquake (GMT +8).
lon	Epicentral longitude of the earthquake.
lat	Epicentral latitude of the earthquake.
dep	Focal depth of the earthquake in km.
magnitude	Magnitude (M).
intensity	(Macro) epicentral intensity.

Author contributions

Conceptualization, XX and XW; Data curation, GY, XW, GC, JR, KL, and CX; Formal analysis, KD, XX, XW, GY; Funding acquisition, XX, GY and XW; Investigation, XX, XW, GY, GC, XY, HY, and XH; Methodology, GY, XW, KD, 495 GC, JR, KL, and CX; Project administration, XX, GY and XW; Software, KD and XW; Supervision, XX and GY; Validation, XX and XW; Writing, XW and XX. All authors have read and agreed to the published version of the manuscript.

Competing interests

The authors declare that they have no conflict of interest.

Acknowledgements

500 We acknowledge all colleagues who have contributed to the active fault databases in China in the past decades. Many scientists and engineers have participated in active fault surveys and mappings and made efforts to build regional-scale project databases. Their work provided basic high-quality materials.

The Earthquake catalogs are downloaded from the Data Sharing Infrastructure of the National Earthquake Data Center (<http://data.earthquake.cn>). We acknowledge the data support from the “China Earthquake Networks Center, National 505 Earthquake Data Center.”

Financial support

This research work was supported by the National Natural Science Foundation of China (Grant No. 41941016) and Research and Development Program of IG, CEA (Name: active fault data management on a cloud platform).

510 References

Basili R., Valensise G., Vannoli P., Burrato, P., Fracassi, U., Mariano, S., Tiberti, M. M., and Boschi, E.: The Database of Individual Seismogenic Sources (DISS), version 3: summarizing 20 years of research on Italy's earthquake geology, *Tectonophysics*, 453(1-4), 20-43, <https://doi.org/10.1016/j.tecto.2007.04.014>, 2008.

515 Basili R., Burrato P., De Santis G. M., Fracassi, U., Maesano, F. E., Tarabusi, G., and DISS Working Group.: Database of Individual Seismogenic Sources (DISS), Version 3.3. 0: A compilation of potential sources for earthquakes larger than M 5.5 in Italy and surrounding areas, <https://doi.org/10.13127/diss3.3.0>, 2021.

CEFIS (V1): <http://www.neotectonics.cn/arcgis/apps/webappviewer/index.html?id=3c0d8234c1dc43eaa0bec3ea03bb00bc>, last access: 27 Nov 2021.



- 520 CEFIS (V2):
<https://data.activetectonics.cn/arcportal/apps/webappviewer/index.html?id=684737e8849c4170bbca14447608c451>, last access: 12 May 2023.
- CAFD WFS: http://data.activetectonics.cn/arcserver/services/Hosted/CAFD400_2022_WFS/MapServer/WFSServer, last access: 12 May 2023.
- 525 CAFD WMS: https://data.activetectonics.cn/arcserver/services/ActiveFaultChinese/CEFSL_CE/MapServer/WMSServer, last access: 12 May 2023.
- Chai, C., Meng, G., Du, P., Wang, Y., Liu, B., Shen, W., Lei, Q., Liao, H., Zhao, C., Fan, S., Zhang, X., and Xie, X.: Comprehensive multi-level exploration of buried active fault: an example of Yinchuan buried active fault, *Seismology and Geology*, 28(4), 536, 2006 (in Chinese).
- 530 Chen, G., Xu, X., Yu, G., An, Y., Yuan, R., Guo, T., Gao, X., Yang, H. and Tan, X.: Co-seismic slip and slip partitioning of multi-faults during the MS8.0 2008 Wenchuan earthquake, *Chinese J. Geophys.-Ch.*, 52(5), 1384-1394, <https://doi.org/10.3969/j.issn.0001-5733.2009.05.028>, 2009.
- Chai, C., Meng, G. and Ma, G.: Active fault survey and earthquake hazard assessment in Yinchuan, Science Press, ISBN 978-7-03-030701-9, 2011 (in Chinese).
- Chen, Y.: Active fault survey and earthquake hazard assessment in Tianjin, Science Press, ISBN 978-7-03-037079-2, 2013.
- 535 Chen, G., Xu, X., Wen, X., and Chen, Y.: Late Quaternary Slip-rates and Slip Partitioning on the Southeastern Xianshuihe Fault System, Eastern Tibetan Plateau, *Acta Geol. Sin.-Engl.*, 90(2), 537-554, <https://doi.org/10.1111/1755-6724.12689>, 2016.
- Chen, J., Rong, Y., Harold, M., Chen, G., and Xu, X.: An Mw-Based Historical Earthquake Catalog for Mainland China, *B. Seismol. Soc. Am.*, 107(5), 2490–2500, <https://doi.org/10.1785/0120170102>, 2017.
- 540 DB/T 53-2013 Mapping of active fault in 1:50 000, recommended standard by China Earthquake Administration, 2013 (in Chinese).
- DB/T 65-2016 Code of 1:50 000 active fault mapping database, recommended standard by China Earthquake Administration, 2016 (in Chinese).
- 545 DB/T 81-2020 Active fault survey-Paleoseismic trenching, recommended standard by China Earthquake Administration, 2020 (in Chinese).
- DB/T 82-2020 Active fault survey-Field geological investigation, recommended standard by China Earthquake Administration, 2020 (in Chinese).
- DB/T 83-2020 Active fault survey-Inspection of database, recommended standard by China Earthquake Administration, 2020 (in Chinese).
- 550 Deng, Q., Zhang, P., Ran, Y., Yang, X., Min, W., and Chu, Q.: Basic characteristics of active tectonics in China, *Sci. China Ser. D.*, 32(1), 1020-1030, <https://doi.org/10.1360/zd2002-32-12-1020>, 2002 (in Chinese).
- Deng, Q., Zhang, P., Ran, Y., Yang, X., Min, W., and Chu, Q.: Basic characteristics of active tectonics of China, *Sci. China Ser. D.*, 46(4), 356-372, <https://doi.org/10.1360/03yd9032>, 2003 (in Chinese).



- 555 Deng, Q., Ran, Y., Yang, X., Min, W., and Chu, Q.: The active tectonic map of China (1:4 000 000), Seismological Press, ISBN 978-7-50-283051-9, 2007 (in Chinese).
- Emre, Ö., Duman, T. Y., Özalp, S., Şaroğlu, F., Olgun, Ş., Elmacı, H., and Çan, T.: Active fault database of Turkey. *B. Earthq. Eng.*, 16(8), 3229-3275, <https://doi.org/10.1007/s10518-016-0041-2>, 2018.
- Earthquake sequence data from NEDC: <https://data.earthquake.cn/gcywfl/index.html>, last access: 20 Jan 2023.
- 560 GB/T 18306-2015 Seismic ground motion parameters zonation map of China, mandatory standard of China, 2015 (in Chinese).
- GB/T 36072-2018 Surveying and prospecting of active fault, mandatory standard of China, 2018 (in Chinese).
- Ganas A., Oikonomou I. A., and Tsimi C.: NOAfaults: A digital database for active faults in Greece. *B. Geol. Soc. Greece*, 47(2), 518-530, 2013.
- GB18306: <http://www.gb18306.net/detail/50>, last access: 20 Jan 2023.
- 565 Geology Institute of China Earthquake Administration (GICEA), Seismotectonic map of China (1:4 000 000), 1979 (in Chinese).
- Gu, G.: Earthquake catalogue of China (from 1831 BC to 1969 AD), Science Press, ISBN 13031·2238, 1983 (in Chinese).
- Guo P., Han Z., Dong S., Mao, Z., Hu, N., Gao, F., and Li, J.: Latest quaternary active faulting and paleoearthquakes on the southern segment of the Xiaojiang fault zone, SE Tibetan plateau, *Lithosphere*, 2021(1), <https://doi.org/10.2113/2021/7866379>, 2021.
- 570 Haller, K. M., Machette, M. N., Dart, R. L., and Rhea, B. S.: U.S. Quaternary fault and fold database released, *Eos, Transactions American Geophysical Union*85(22), 218-218, <https://doi.org/10.1029/2004EO220004>, 2004.
- Hou, K.: Active fault survey and earthquake hazard assessment in Nanjing, Seismological Press, ISBN 978-7-50-283971-0, 2012 (in Chinese).
- 575 He, F., Bai, L., Wang, J., Liu, Y., Cai, X., Sun, Y., Zhang, L., Fang, T., and Guo, G.: Deep structure and quaternary activities of the Xiadian fault zone, *Seismology and Geology*, 35(3), 490-505, <https://doi.org/10.3969/j.issn.0253-4967.2013.03.004>, 2013.
- Huang, X., Yang, X., Yang, H., Hu, Z., and Zhang, L.: Re-Evaluating the Surface Rupture and Slip Distribution of the AD 1609 M7 1/4 Hongyapu Earthquake Along the Northern Margin of the Qilian Shan, NW China: Implications for Thrust Fault Rupture Segmentation, *Front. Earth Sc.-Switz*, 9, 98, <https://doi.org/10.3389/feart.2021.633820>, 2021a.
- 580 Huang, X., Yang, H., Yang, X., Yang, H., Hu, Z., and Zhang, L.: Holocene paleoseismology of the Fodongmiao-Hongyazi Fault along the Northern Tibetan margin (Western China) and implication to intraplate earthquake rupturing pattern, *Tectonophysics*, 808, 228812, <https://doi.org/10.1016/j.tecto.2021.228812>, 2021b.
- 585 Liu, B., Chai, C., Feng, S., Zhao, C., Yuan, H.: Seismic exploration method for buried fault and its up-breakpoint in Quaternary sediment area—An example of Yinchuan buried active fault, *Chinese Journal of Geophysics*, 51(5), 1475-1483, 2008 (in Chinese).



- Lei, Q., Chai, C., Meng, G., Du, P., Wang, Y., Xie, X., Zhang, X.: Composite drilling section exploration of Yinchuan buried fault, *Seismology and Geology*, 30(1), 250-263, 2008 (in Chinese).
- 590 Liang, G. and Wu, Y.: Active fault survey and earthquake hazard assessment in Guangzhou, Science Press, ISBN 978-7-03-037757-9, 2013 (in Chinese).
- Langridge, R. M., Ries, W. F., Litchfield, N. J., Villamor, P., Van Dissen, R. J., Barrell, D. J. A., Rattenbury, M. S., Herona, D. W., Haubrocka, S., Townsenda, D. B., Leea, J. M., Berrymana, K. R., Nicolc, A., Cox S. C., Stirling, M. W.: The New Zealand active faults database. *New Zeal. J. Geol. Geop.*, 59(1), 86-96, <https://doi.org/10.1080/00288306.2015.1112818>, 2016.
- 595 Li, K., Xu, X., Wei, L., Wang, Q., and Shu, P.: Evidence of long recurrence times and low slip rate along the 1668 Tancheng earthquake fault, *Chin Sci Bull*, 64, 1168–1178, <https://doi.org/10.1360/N972018-00961>, 2019.
- Ma, X.: Lithospheric dynamics map of China and adjacent sea area (1:4 000 000), 1987 (in Chinese).
- Maldonado, V., Contreras, M., Melnick, D.: A comprehensive database of active and potentially-active continental faults in Chile at 1: 25,000 scale. *Sci. data*, 8(1), 1-13, <https://doi.org/10.6084/m9.figshare.13268993>, 2021.
- 600 Nation-scale earthquake intensity zonation map compiling team (NEIZMT): Spatial distribution map of active tectonics and strong earthquakes in China (1:3 000 000), China Earthquake Administration, 1976 (in Chinese).
- Nation-scale earthquake intensity zonation map compiling team (NEIZMT): Map of the major tectonic-system activity and strong earthquakes epicentre distribution in China (1:6 000 000), China Earthquake Administration, 1978 (in Chinese).
- NEDC: <https://data.earthquake.cn/zcfg/index.html>, last access: 20 Jan 2023.
- 605 NEDC (sub-center in IG, CEA): <http://datashare.igl.earthquake.cn/map/ActiveFault/introFault.html>, last access: 20 Jan 2023.
- Qu C.: Building to the active tectonic database of China, *Seismology and Geology*, 30 (1), 298-304, 2008 (in Chinese).
- Rong, Y., M.EERI, Xu, X., Jia Cheng, J., Chen, G., Magistrale, H., M.EERI, and Shen, Z.: A probabilistic seismic hazard model for Mainland China, *Earthq. Spectra*, 36(1_suppl), 181-209, <https://doi.org/10.1177/8755293020910754>, 2020
- 610 Shen, J. and Bo, J.: Active fault survey and earthquake hazard assessment in Songyuan, Seismological Press, ISBN 978-7-5028-4731-9/P(5427), 2016 (in Chinese).
- Shu, P., Fang, L., Zheng, Y., Lu, S., Pan, H., Song, F., and Li, S.: Geological Evidence and Characteristics of Activity of the Wuhe-Mingguang Section of Tancheng-Lujiang Fault Zone in Late Pleistocene, *Earthquake Research in China*, 30(4), 485-499, 2016.
- 615 Sun, H., He, H., Wei, Z., Shi, F. and Gao, W.: Late Quaternary paleoearthquakes along the northern segment of the Nantinghe fault on the southeastern margin of the Tibetan Plateau. *J. Asian Earth Sci.*, 138, 258-271, <https://doi.org/10.1016/j.jseaes.2017.02.023>, 2017.
- Shi F., He H., Gao W., Sun, H., Wei, Z., Hao, H., Zou J., Sun, W., and Su, P.: Holocene paleoearthquakes on the Tianqiaogou-Huangyangchuan fault in the northeastern boundary fault system of the Tibetan Plateau, *J. Asian Earth Sci.*, 186, 104049, <https://doi.org/10.1016/j.jseaes.2019.104049>, 2019.



- 620 Shu, P., Min, W., Liu, Y., Xu, X., Li, K., Yu, Z., Yang, H., Luo, H., Wei, S., and Fang, L.: Late Quaternary paleoseismology and faulting behavior of the Yilan-Yitong fault zone and implications for seismic hazards of the Tanlu fault zone, eastern China. *J. Asian Earth Sci.*, 201,1-18, <https://doi.org/10.1016/j.jseaes.2020.104509>, 2020.
- Shi F., He H., Liu Y., Wei, Z., and Sun, H.: Active Tectonics of the Nantinghe Fault in Southeastern Tibetan Plateau and its Implications for Continental Collision. *Front. Earth Sci.*, 9, 818225, <https://doi.org/10.3389/feart.2021.818225>, 2022.
- 625 Trifonov, V. G.: Active faults in Eurasia: general remarks, *Tectonophys.*, 380, 123–130, <https://doi.org/10.1016/j.tecto.2003.09.017>, 2004.
- Tian, S.: Faults Investigation and Evaluation for Seismic Safety Assessment of Nuclear Power Plants, *Technology for Earthquake Disaster Prevention*, 1(1), 25-30, <https://doi.org/10.3969/j.issn.1673-5722.2006.01.004>, 2006 (in Chinese).
- 630 Valensise, G. and Pantatosti, D., Database of potential sources for earthquakes larger than M 5.5 in Italy. Version 2.0-2001. Italy: N. p., 2001. Web.
- Wang, Y., Meng, G., Chai, C., Liu, Q., Du, P., and Xie, X.: The accurate location methods of buried active fault exploration: an example of Luhuatai faults in Yinchuan graben, *Seismology and Geology*, 37(1), 256, <https://doi.org/10.3969/j.issn.0253-4967.2015.20>, 2016 (in Chinese).
- 635 Wu, Z., Zhou, C., Ma, X., Wang, J., Huang, X., Wu, X., Hu, M., Ha, G., and Liu, J.: Active faults map of China and adjacent seas (1:5 000 000), Geological Publishing House, 2018 (in Chinese).
- Wu, X., Du, K., Yu G., Chen, G., Dong, Y., Xu, X., Chen, Z., and Xu, C.: Implementation and future challenges of seismotectonic mapping system for earthquake emergency response, In *IOP Conference Series: Earth and Environmental Science*, 861(5), p. 052047, 2021.
- 640 Williams, J. N., Wedmore, L. N., Scholz, C. A., Kolawole, F., Wright, L. J., Shillington, D. J., Åke Fagereng, Biggs J., Mdala H., Dulanya Z., Mphepo F., Chindandali P. R. N., Werner, M. J.: The Malawi Active Fault Database: An Onshore - Offshore Database for Regional Assessment of Seismic Hazard and Tectonic Evolution. *Geochem., Geophys., Geos.*, 23(5), e2022GC010425, <https://doi.org/10.1029/2022GC010425>, 2022.
- 645 Wu, X., Xu, C., Xu, X., Chen, G., Zhu, A., Zhang, L., Yu, G., and Du, K.: A Web-GIS hazards information system of the 2008 Wenchuan Earthquake in China, 2, 210-217, *Natural Hazards Research*, <https://doi.org/10.1016/j.nhres.2022.03.003>, 2022.
- Xu, X. and Deng, Q.: Nonlinear characteristics of paleoseismicity in China. *Journal of Geophysical Research: Solid Earth*, 101(B3), 6209-6231, <https://doi.org/10.1029/95JB01238>, 1996.
- Xu, X., Ji, F., Yu, G., Chen, W., Wang, F., and Jiang, W.: Reconstruction of paleoearthquake sequence using stratigraphic records from drill logs: a study at the Xiadian Fault, *Seismology and Geology*, 22(1), 9-19, 2000 (in Chinese).
- 650 Xu, X., Yu, G., Ma, W., Ran, Y., Chen, G., Han, Z., Zhang, L., and You, H.: Evidence and methods for determining the safety distance from the potential earthquake surface rupture on active fault, *Seismology and Geology*, 24(4), 470-483, 2002 (in Chinese).
- Xu, X.: Active Faults, Associated Earthquake Disaster Distribution and Policy for Disaster Reduction, *Technology for Earthquake Disaster Prevention*, 1(1):7-14, <https://doi.org/10.3969/j.issn.1673-5722.2006.01.002>, 2006 (in Chinese).



- 655 Xu, Z., Ji, S., Li, H., Hou, L., Fu, X., and Cai, Z.: Uplift of the Longmenshan range and the Wenchuan earthquake, Episodes, 31, 291-301. <https://doi.org/10.18814/epiiugs/2008/v31i3/002>, 2008a.
- Xu, X., Wen X., Ye J., Ma B., Chen, Zhou, et al, The MS 8.0 Wenchuan Earthquake surface ruptures and its seismogenic structure, Seismology and Geology, 30(3), 597-629, 2008b (in Chinese).
- 660 Xu, X., Wen, X., Yu, G., Chen, G., Klinger, Y., Hubbard, J., and Shaw, J.: Coseismic reverse- and oblique-slip surface faulting generated by the 2008 Mw 7.9 Wenchuan earthquake, China, Geology, 37(6), 515-518, <https://doi.org/10.1130/G25462A.1>, 2009a.
- Xu, X.: Album of 5.12. Wenchuan MS 8.0 earthquake surface ruptures, China, Seismological Press, ISBN 978-7-5028-3542-2, 2009b (in Chinese).
- 665 Xu, X., Jiang, G., Yu, G., and Wu X., Zhang J., and Li X.: Discussion on seismogenic fault of the Ludian M_S 6.5 earthquake and its tectonic attribution, Chinese Journal of Geophysics, 57(9), 3060-3068, <https://doi.org/10.6038/cjg20140931>, 2014a (in Chinese).
- Xu, C., Xu, X., Shen, L., Dou, S., Wu, S., Tian, Y., and Li, X.: Inventory of landslides triggered by the 2014 M_S 6.5 Ludian earthquake and its implications on several earthquake parameters, Seismology and Geology, 36(004), 1186-1203, <https://doi.org/10.3969/j.issn.0253-4967.2014.04.020>, 2014b (in Chinese).
- 670 Xu, X., Yu, G., Ran, Y., Yang, X., Zhang, L., Sun, F., Du, W., and Liu, B.: Introduction on urban active faults in China: urban active fault survey achievement in 20 large cities of China, Seismological Press, ISBN 978-7-5028-4410-3, 2015 (in Chinese).
- Xu, X., Guo T., Liu S., Yu G., Chen G., Wu X.: Discussion on issues associated with setback distance from active fault. Seismology and Geology, 38(003), 477-502, <https://doi.org/10.3969/j.issn.0253-4967.2016.03.001>, 2016a (in Chinese).
- 675 Xu, X., Han, Z., Yang, X., Zhang, S., Yu, G., Zhou, B., Li, F., Ma, B., Chen, G., and Ran, Y.: Seismotectonic Map in China and its Adjacent Regions (1:4 000 000), Seismological Press, 2016b (in Chinese).
- Xu, X., Wu, X., Yu, G., Tan X., Li, K.: Seismo-Geological Signatures for identifying M_≥7.0 earthquake risk areas and their preliminary application in mainland China, Seismology and Geology, 39(002), 219-275, <https://doi.org/10.3969/j.issn.0253-4967.2017.02.001>, 2017 (in Chinese).
- 680 Xu, X.: China Active Fault Database, Active Fault Survey Data Centre at Institute of Geology, China Earthquake Administration [data set], <https://doi.org/10.12031/activefault.china.400.2022.db>, 2022.
- Yang, F.: Active fault survey and earthquake hazard assessment in Changchun, Seismological Press, ISBN 978-7-5028-3695-5, 2010 (in Chinese).
- 685 Yoshioka, T., and Miyamoto, F.: Active fault database of Japan: Its construction and search system. In AGU Fall Meeting Abstracts, Vol. 2011, pp. S21A-2144, 2011.
- Yang, H., Yang, X., Huang, X., Li, A., Huang, W., and Zhang, L.: New constraints on slip rates of the Fodongmiao-Hongyazi fault in the Northern Qilian Shan, NE Tibet, from the 10Be exposure dating of offset terraces, J. Asian Earth Sci., 151, 131-147, <https://dx.doi.org/10.1016/j.jseaes.2017.10.034>, 2018a.



- 690 Yang, H., Yang, X., Zhang, H., Huang, X., Huang, W., and Zhang, N.: Active fold deformation and crustal shortening rates of the Qilian Shan Foreland Thrust Belt, NE Tibet, since the Late Pleistocene. *Tectonophysics*, 742, 84-100, <https://doi.org/10.1016/j.tecto.2018.05.019>, 2018b.
- Yang, H., Yang, X., Huang, W., Li, A., Hu, Z., Huang, X., and Yang, H.: ¹⁰Be and OSL dating of Pleistocene fluvial terraces along the Hongshuiba River: Constraints on tectonic and climatic drivers for fluvial downcutting across the NE Tibetan Plateau margin, China, *Geomorphology*, 348, 106884, <https://doi.org/10.1016/j.geomorph.2019.106884>, 2020.
- 695 Yeats, R. S., K. Sieh, C. R. Allen: *The Geology of Earthquakes*, Oxford: Oxford University Press, 1997.
- Zelenin, E., Bachmanov, D., Garipova, S., Trifonov, V., and Kozhurin, A.: The Active Faults of Eurasia Database (AFEAD): the ontology and design behind the continental-scale dataset, *Earth Syst. Sci. Data*, 14, 4489–4503, <https://doi.org/10.5194/essd-14-4489-2022>, 2022.
- 700 Zhu, J., Xu, X., and Huang, Z.: Active fault survey and earthquake hazard assessment in Fuzhou, Science Press, <https://doi.org/10.3969/j.issn.1001-4683.2005.01.001>, 2005 (in Chinese).
- Zhang, P., Deng, Q., Zhang, G., Ma, J., Gan, W., Min, W., Mao, F., and Wang, Q.: Active tectonic blocks and strong earthquakes in the continent of China, *Sci. China Ser. D*, 46(2), 13-24, 2003.